

## Five Parameter PV Model Extraction and Improvement Based on Experimental Data

Ali M. Humada<sup>1,2</sup>, Mojgan Hojabri<sup>1</sup>, Mohd Herwan Bin Sulaiman<sup>1</sup>, Saad Mekhilef<sup>3</sup>

<sup>1</sup>Faculty of Electrical and Electronics Engineering, University Malaysia Pahang, Pekan, Malaysia <sup>2</sup>Electricity Production Directorate of Salahaldeen, Ministry of Electricity, Salahaldeen, Iraq.

<sup>3</sup>Power Electronics and Renewable Energy Research Laboratory (PEARL), Department of Electrical Engineering, University of Malaya, Kuala Lumpur, Malaysia

### Abstract

This paper presents a new approach of the single diode five parameters model extraction and performance evaluation. The proposed model is capable of analytically describing the I–V and P–V characteristics of a PV module in different conditions. The PV parameters identify, mainly, the accuracy of any PV model. The proposed model constructed in a method to be in a sounds level of accuracy and far from complication. In term of accuracy, different evaluation criteria have being used in this study, and results of all criteria showed merit level of accuracy comparison to those in the compared models. In addition, the performance of the five parameters has been improved and this improvement showed in the I–V and P–V characteristics. Effect of these five parameters on all of the maximum power point (MPP), short circuit current ( $I_{sc}$ ), and open circuit voltage ( $V_{oc}$ ) also showed in the results. The outcomes of this study could help in improving the total PV system performance and could be a guide for method of extraction the five parameters model, since it dependent mainly on real results.

**Keywords:** PV modeling; five parameters; parameters extraction; maximum power point; PV characteristics.

### Introduction

Solar energy is considered as green and clean energy source, because it has marginal environmental and health impacts compared to fossil fuels. In addition, the fast decline in the photovoltaic (PV) modules cost, and on the other hand, the acceleration in the price of petrochemical fuels, besides it is going to drain. All these things have motivated the diffusion of PV solar systems that, in the past, were considered attractive only for special applications in faraway and isolated regions.

Collection of this energy and converting it into the most useful way like electrical power for daily usages is an exquisite; nonetheless the technologies have its own boundaries and difficulties which must be resolved in advance of photovoltaic (PV) implementation on a large scale. In the frontline of these difficulties are PV system modeling and characterization at an accurate way is requisite in the system design [1, 2].

The PV modeling has posed a challenge for researchers in order to achieve a precise model which strictly emulates the characteristics of PV system within specified or non-specified climate conditions. The important factor could control the model accuracy is the accurateness of extracted parameters of a model. In addition, the number of parameters used in such a model is directly related to model accuracy, the five parameter model is the most accurate one among others [3].

Recently, many researchers conducted their researches on PV modeling and parameters extraction based on different number of PV parameters. In Ref. [4], an approach to find model parameters for single-diode model of PV panel proposed. The influence of both irradiation and temperature on these parameters was considered. But, methods to find the model parameters in case of instantaneous variation in temperatures and irradiances have not been considered and argued. In another study [5], PV modeling was built upon simple procedures to acquire PV system parameters in an easy and fast method. This model was used mainly to characterize these parameters by using MATLAB/ Simulink. Nonetheless, applicability of using this model is limited since the model didn't consider fast climate change. Later, in Ref. 2014, modeling improvement of the four parameter model was conducted [6]. Therefore, this study was conducted to build a model able to fit the variation of the current voltage characteristics (I-V) under various operating conditions. However, lack of practical analysis in this study made the validation weak. Improvement modeling technique in Ref. [7] is based on genetic algorithm optimization with number of PV panel parameters which figured through this approach. Modeling was executed in two, single diode model and double diode model. Based on this study, the single diode model is more efficient than a double diode model. Meanwhile, another study [8] offered an improved PV system modeling technique via differential evolution (DE) algorithm. This method enables a special capability of computing all PV parameters at any irradiance and temperature values. Nevertheless, it has computational steps in the computation process.

In this paper, modeling and characterization for a 5 kWp grid-connected PV system installed in Malaysia has done. As a worthwhile contribution of this study, an accurate global PV model is provided. Eventually, a precise characterization is accomplished based on practical data and the

legacy works. It is therefore expected that this study could be a reference for those are interesting in PV modeling and installation under fluctuated climatic conditions.

## 2. Modeling and Characterization of PV System

PV system modeling and characterization, as introduced in the first part, is a vital link of any improvement of PV system characteristics, which finally lead to improve the characteristics of the energy extracted from that system. In this purpose, methodology of PV system modeling and characterization is introduced and verified with real data in current study. Five parameters model is used in this research to characterize the PV array. Based on realistic parameters driven from mathematical calculations, an accurate mathematical model for the PV system is derived and its performance evaluated.

### 2.1 PV System Modeling

The single-diode PV model is the base of implementing the proposed PV model, as shown in Figure 1. The modeling of any PV cell or module encompasses the step calculations of both; current–voltage (I–V) and power–voltage (P–V) characteristics based on precise formula. Meanwhile, it is difficult and challenge task to construct a model represents different levels of the irradiance and the temperature, which could be help in estimating the parameters in a truly and representative method [9, 10]. Furthermore, controlling the quality of solar cells and evaluating the performance of photovoltaic (PV) systems are directly related to the accuracy level of measurement of the I–V and P–V characteristics. Nonetheless, accuracy of such measurement is mainly depending on the number of solar cell parameters extracted in such a model. The studies in the literature are varied in the application of a number of parameters used in building its models. Some researchers built those models based on five parameter model, while others built the PV model based on four, three, two, or even one parameter model. However, the five-parameter model is the most widely used model and most accurate one, particularly for outdoor condition tests [11, 12]. Thus, it should be equipped with better accuracy by taking into consideration all of the available DC parameters.

Therefore, this study implemented based on the single-diode, five- parameter model. The conventional equation below describes a simple single-diode model with distinctive I–V characteristics:

$$I = I_{ph} - I_o \left[ \exp\left(\frac{IR_s}{a}\right) - 1 \right] - \frac{IR_s}{R_{sh}} \quad (1)$$

where  $I_{ph}$  is the photocurrent,  $I_o$  is the reverse saturation current of the diode,  $a$  is the modified ideality factor,  $R_s$  series resistance, and  $R_{sh}$  is the parallel resistance. The proposed equations of the existing parameters are presented in the next part.

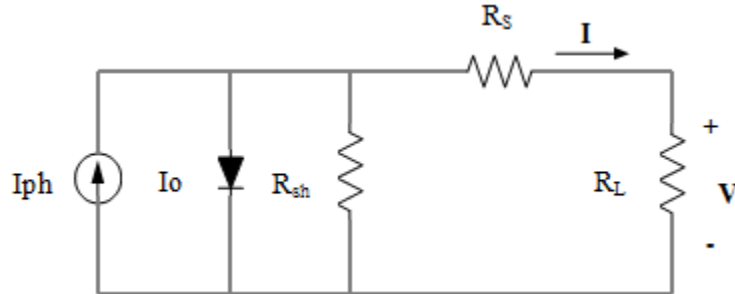


Fig. 1. Single-diode model equivalent circuit.

## 2.2 PV System Characterization

Based on the general definition of PV modeling, the current–voltage (I–V) and power–voltage (P–V) characteristics of solar cells/modules have the most importance in the photovoltaic industry because it exactly reflects the cell/module performance. However, it is not straightforward to get the model parameters from these (I–V) and (P–V) curve for photovoltaic (PV) cells/modules [13, 14]. For example, the (I–V) and (P–V) characteristics of the single-diode model affect by the cell temperature and the irradiance value mainly, besides to the effect of the five electric parameters.

In this work, experimental data for a PV system installed under Malaysia climate condition were employed to characterize the PV models and its parameters, and then to develop an accurate values for the coefficient constants;  $C_1$  to  $C_9$  (coefficient of the equations of the five-parameter used in this study). These nine coefficients are part of the PV parameters formula in this study, which benefits in utilizing an accurate global PV model.

The ideality factor ( $n$ ) usually ranged between 1 and 2 (although it might be greater in very few situations), which depends on the construction method and semiconductor material. Generally, the proposed PV system model is from five parameters model which namely  $I_L$ ,  $I_o$ ,  $a$ ,  $R_s$ , and  $R_{sh}$ . This model can be used for an individual cell, for a module consisting of several cells, or for an array consisting of several modules.

Nonetheless, due to the difficulty in finding the accurate value of  $n$ , assume that:

$$C_1 = \frac{q}{nk} \quad (2)$$

Then

$$a = \frac{T_c}{C_1} \quad (3)$$

Usually, the light generation-current ( $I_L$ ) is proportional to the value of solar irradiation as well as it is supposed to be linearly dependent on the effective cell temperature ( $T$ ) [15]. Consequently, this light generation-current could be stated as:

$$I_L = (C_2 + C_3 \cdot T - C_4) \cdot G \quad (4)$$

In a related literature [16], researchers proved that the cell temperature ( $T$ ) is affecting the diode saturation current,  $I_o$  in a linear mode, and the effectiveness of  $I_o$  is shown in Eq. (3.7).

$$I_o = C_5 \cdot T^3 \cdot \exp\left(-\frac{C_6}{T}\right) \quad (5)$$

On the other hand, the series resistance ( $R_S$ ) is mainly depends and proportional to the value of effective cell temperature ( $T$ ) [17]. Accordingly, this series resistance could be defined as:

$$R_S = C_7 - \frac{C_8}{T} \cdot \exp\left(-\frac{T}{C_9}\right) \quad (6)$$

Where the value of  $C_7$  it is presented and called as  $R_{So}$  which can be found from the slope at open-circuit point, or called open circuit voltage ( $V_{oc}$ ), as follows:

$$R_{So} = -\left(\frac{dv}{di}\right)_{V_{oc}} \quad (7)$$

Whereas the value of  $R_{Sh}$  can be found directly from the slope at short-circuit point, or called short circuit current ( $I_{sc}$ ), as follows:

$$R_{Sh} = R_{Sho} = -\left(\frac{dv}{di}\right)_{I_{sc}} \quad (8)$$

Where,  $C_1$ – $C_9$  are coefficients,  $G$  is the value of solar irradiance, and  $T$  is the value of temperature of the cell.

In the current study, the attained experimental outcomes have been applied to estimation precise values of the constant coefficients  $C_1-C_9$ . Nevertheless, due to the continues changing in the climate conditions (like the irradiance and temperature) straightaway changes, therefore the values of the voltage and current registers and saved every 1 second.

These data include actual values for all of the parameters  $a$ ,  $I_L$ ,  $I_o$ ,  $R_s$ , and  $R_{sh}$  used. The experimental values of these parameters are then used to obtain the constant coefficient values ( $C_1-C_9$ ) and then to find the theoretical values in the purpose of attaining precise values of the constant coefficients ( $C_1-C_9$ ).

The values of these constants ( $C_1$  to  $C_9$ ) are presented in Table 2. The selected system consisted of 5 kW grid-connected PV systems, which has been investigated through the simulation for a month (from 01.05.2014 to 31.05.2014) and its specification presented in Table1. Throughout this period, irradiancies, cell temperatures, output current, output voltage and PV output power are recorded for every 1 second.

Table 1. Specifications of the proposed system.

Parameter	Value and Units
Number of PV modules	23 PCs
Maximum Power ( $P_{MP}$ )	216 Watts
Maximum Voltage ( $V_{MP}$ )	24.10 Volts
Maximum Current ( $I_{MP}$ )	8.952 Amps
Open Circuit Voltage ( $V_{oc}$ )	24.5 Volts
Short Circuit Current ( $I_{sc}$ )	9.05 Amps

These constant values ( $C_1-C_9$ ) are derived in different illumination levels, which are estimated accurately based on gained experimental results as presented in Table 2.

Table. 2. Shows C1to C9 coefficient values

Factor	Value
C1	0.0059
C2	0.0047
C3	6.732E-6
C4	3.219E-8
C5	2.663E-4
C6	6318
C7	4.11
C8	118
C9	3517

As mentioned above, this work has focused on all the available five DC electric parameters  $n$ ,  $I_L$ ,  $I_o$ ,  $R_s$ , and  $R_{sh}$ . In other works such as Ref. [5], the characteristics are based on only two parameters  $n$  and  $I_L$ . While, in other research works [6–8], the model is depends only on the equations for  $I_L$  and  $I_o$ . Furthermore, the current work targets to originate new parameters within fluctuated weather conditions (Malaysia as the case study) which might be applicable globally and for all fluctuated climate. As a result, set of new equations based on the extracted values can be derived as below.

$$a = \frac{T_c}{0.0059} \quad (9)$$

$$I_L = (0.0047 + 6.732E^{-6} \cdot T - 3.219E^{-8})G_T \quad (10)$$

$$I_o = 2.663E^{-4} - 4 \cdot T^3 \cdot \exp\left(-\frac{6318}{T}\right) \quad (11)$$

$$R_s = 4.11 - \frac{118}{T} \cdot \exp\left(-\frac{T}{3517}\right) \quad (12)$$

Different evaluation criteria were used to validate the results of these parameters of the proposed model and compared it with other models from the literature. The validation was done with the most used and famous parameters of evaluations. Also, as shows in Table 3, the validation was done between the relations of the five parameters ( $I_L$ ,  $I_o$ ,  $a$ ,  $R_s$  and  $R_{sh}$ ), which were found in this research and other models found in literature. From these Figures we can see that the equations proposed in the current study for all the calculation of these parameters were more accurate comparing with the equations introduced in [6, 12, 18-21].

In addition to that and from Table 3, the computed coefficients look to be more accurate compared with the other models. Additionally, the proposed equations of the compared models contained of several constants. Consequently, the equations of those models aren't easy. Furthermore, the proposed model is contained from five parameters of the solar cells ( $I_L$ ,  $I_o$ ,  $a$ ,  $R_s$  and  $R_{sh}$ ) which lead to increase its accuracy. Whereas some other studies its models contained from less number of parameters which affect the accuracy of that models, like the study in [22] contained from four parameters or only from three parameters ( $a$ ,  $R_s$  and  $R_{sh}$ ) like in [23]. However, in some studies they have focused on two parameters, like in [24] used the  $R_s$  and parameter  $a$  and in [25] used  $R_s$  and  $R_{sh}$  to in that models, or based on only one parameter which was the  $R_s$  for most one parameter studies like in [15]. Finally, the current study aimed to originate new relations considers the tropical weather condition and this has not been done before.

Generally, validation of this study utilized to confirm the accuracy of the proposed model where it is based on several benchmarks like mean absolute percentage error (MAPE), R-square, SSE, SSR, and SST as stated before. The results of model evaluation of the calculated factors are presented in Table 3.

Thus, the experimental data for these five parameters ( $I_L$ ,  $I_o$ ,  $a$ ,  $R_s$  and  $R_{sh}$ ) is used to estimate accurate and reliable values for the nine constants in this research (C1 to C9) by comparing them with the theoretical results. Nevertheless, due to the rapid and continuous weather fluctuation conditions such as irradiance and temperature, data logging has been accomplished continuously for both current and voltage (every 1 second).

Table 3. Shows results of evaluation criteria of the proposed model

<b>Evaluation Creteria</b>	<b>Parameter <math>A</math></b>	<b>Parameter <math>I_o</math></b>	<b>Parameter <math>I_L</math></b>	<b>Parameter <math>R_s</math></b>	<b>Parameter <math>R_{sh}</math></b>
MAPE	3.12%	4.9%	2.3%	7.3%	11.3%
SSE	2.198E-16	2.721E-15	7.216E-14	4.374E-12	4.345E-11
R-square	0.9998	0.998	0.997	0.995	0.993
SSR	1.09878E-12	1.362E-12	2.3982E-11	8.473E-10	9.872E-9
SST	1.099E-12	1.364E-12	2.405E-11	6.463E-10	4.324E-9



### 3. Results of Effect Temperature and Irradiance on I–V and P–V Characteristics

The above model equations are used to simulate Kyocera KC175GHT PV module in order to test its performance in fitting the I–V and P–V curve at standard test conditions ( $E = 1000 \text{ W/m}^2$  ;  $T = 25 \text{ }^\circ\text{C}$ ). In the first time, with fixing cell temperature ( $25^\circ\text{C}$ ) and changing irradiance values and seeing its characteristics, and in another time fixing the radiance value with  $1000 \text{ W/m}^2$  and changing the temperature values (Kyocera PV module specification details in Table 1). In addition, the author has employed other models [12, 20, 21] from literature to prove the accuracy of the used model comparing to that models with respect to the real results (experimental). Besides to the effect of the temperature and irradiance values, the author attempted to estimate the behavior of a solar panel for different values of solar parameters on the I–V and P–V and the obtained results are compared with those models.

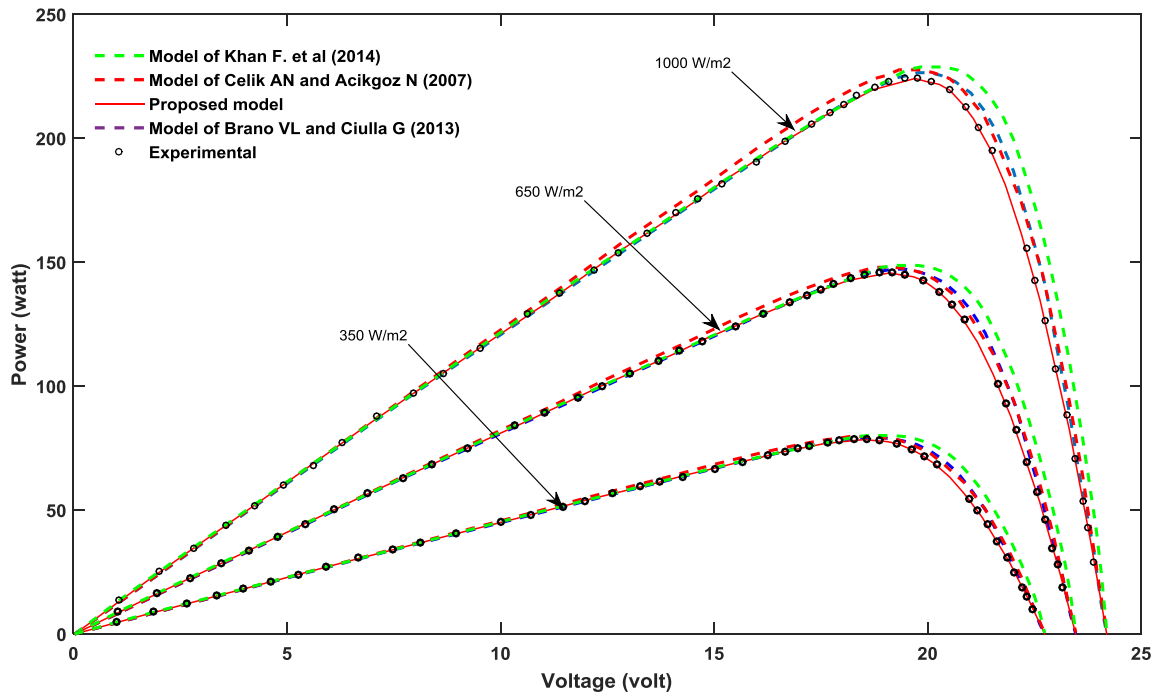


Figure 2. Effect of changing irradiance conditions on the P–V characteristic curve, with fixed cell temperature ( $25^\circ\text{C}$ )

One can see in Figures 2 and 3 that the model fits the I–V and P–V curves at different radiance values and fixed temperature (25C°). The results evident that in both of the I–V and P–V characteristic curves the proposed model is making a smooth convergence with the experimental results more than the other models [12, 20, 21]. Therefore, the accuracy of the proposed model compared with the other models presented in Table 4. In addition, from these two Figures we can notice that all the models affected by the changing of radiance value in the same weight, else model of Brano VL and Ciulla G [21]. In ref. [21], the maximum power point (MPP) is decreased more than the other models with decreasing the radiance, and this is because in this model they proposed that the radiance value effect in a direct way on the MPP rather than the open circuit voltage ( $V_{oc}$ ) and short circuit current ( $I_{sc}$ ).

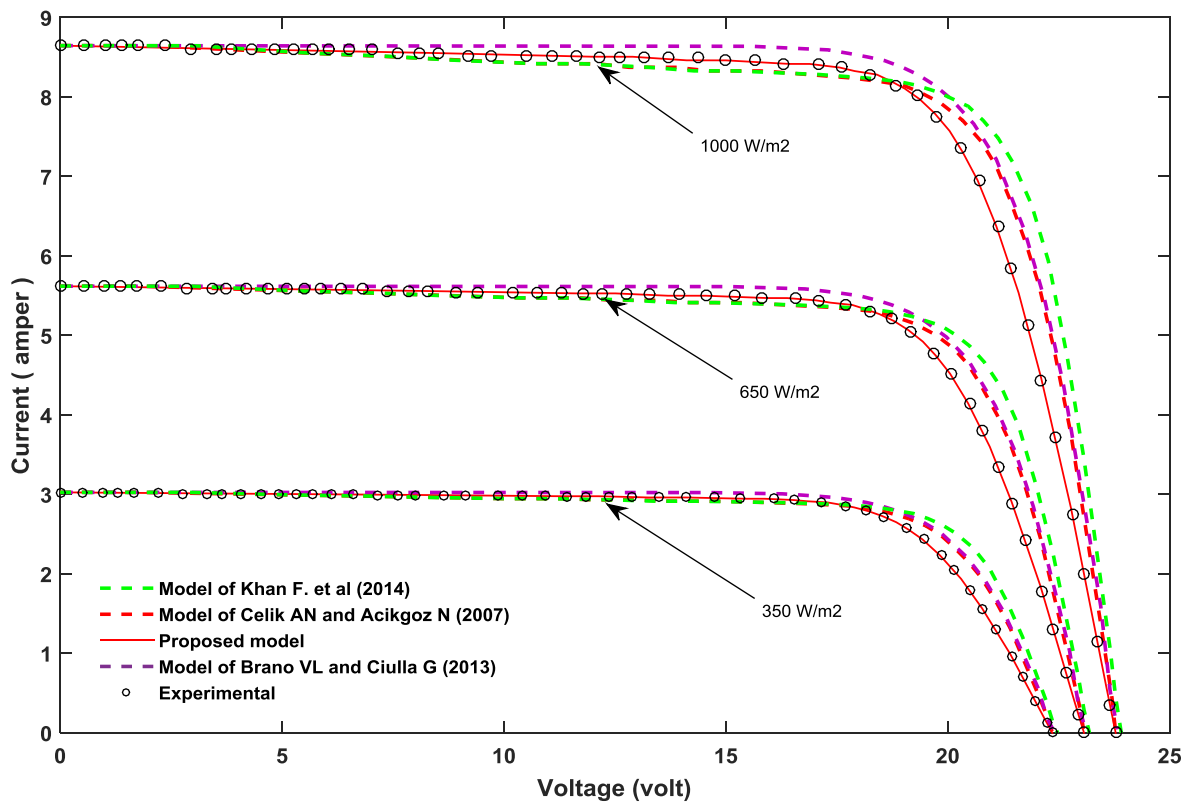


Figure 3. Effect of changing irradiance conditions on the I–V characteristic curve, with fixed cell temperature (25C°)

Furthermore, changing the radiation level has the same weight of effect on both of  $V_{oc}$  and  $I_{sc}$  for all the compared models and the proposed one.

On the other hand, the effect of changing the cell temperature values on the I–V and P–V characteristic curves takes another shape of the effectiveness. The results of the changing cell temperature levels with fixing the irradiance ( $1000 \text{ W/m}^2$ ) presented in Figures 4 and 5, for the P–V and I–V characteristic curves, respectively.

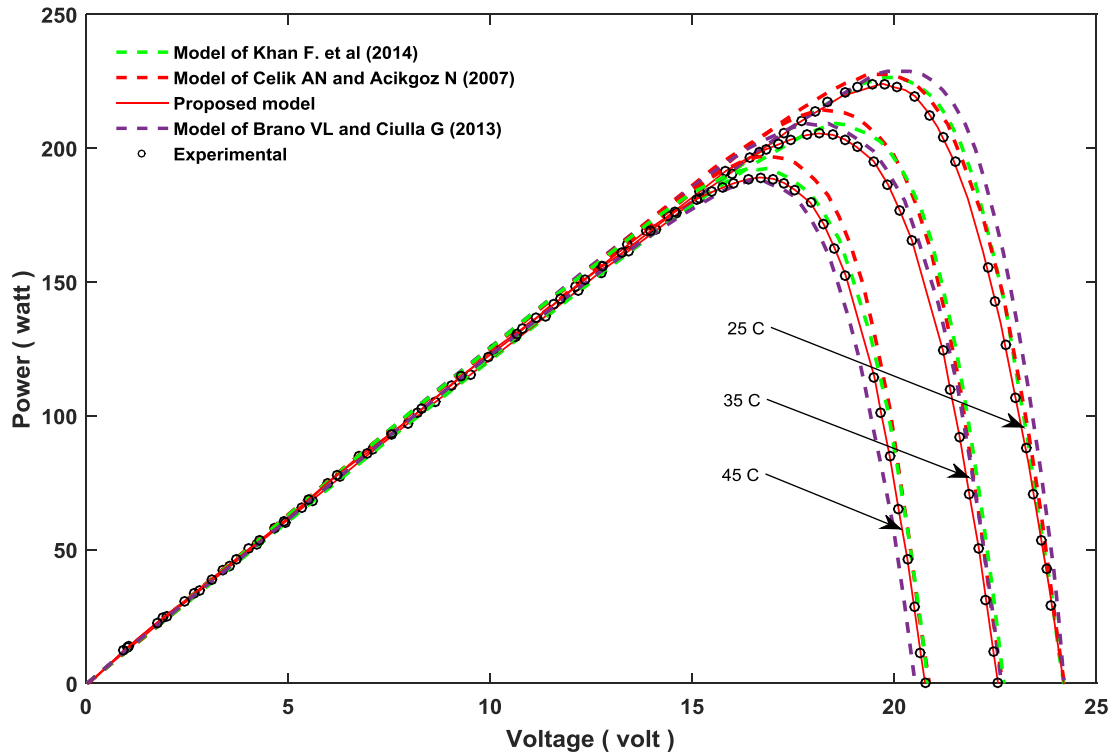


Figure 4. Effect of changing cell temperature on the P–V characteristic curve, with fixed irradiance level ( $1000 \text{ W/m}^2$ ).

Results of Figures 4 and 5 are shown that the model fits the I–V and P–V curves at different cell temperature values and fixed irradiance ( $\text{W/m}^2$ ). These results apparent that in both of the I–V and P–V characteristic curves the proposed model is making a smooth convergence with the experimental results better than the other models [12, 20, 21]. Besides to the good accuracy occurred from the results of irradiance effect, the accuracy of the proposed model within cell temperature effect compared with the other models is also presented in Table 4. In addition, from these two Figures we can notice that all the models affected by the changing of cell temperature values in the same weight, else model of Brano VL and Ciulla G [21]. In [21], the maximum power point (MPP) is decreased more than the other models, and

also more than the ones in case of effect irradiance value, with decreasing the radiance. This is also because of in this model they proposed that the cell temperature value effect in a direct way on the MPP rather than the open circuit voltage ( $V_{oc}$ ) and short circuit current ( $I_{sc}$ ).

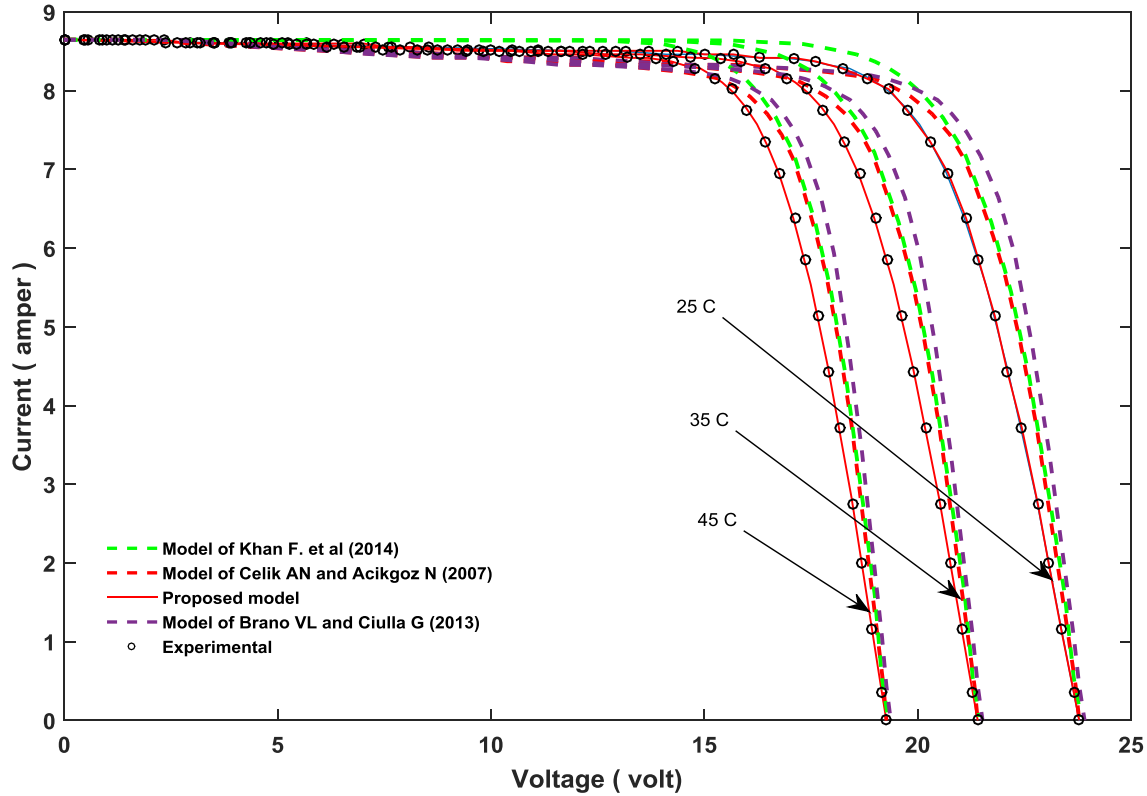


Figure 5. Effect of changing cell temperature on the I–V characteristic curve, with fixed cell temperature (25C°)

#### 4. Results of Effect Solar Cell Parameters On I–V And P–V Characteristics Performance

The equations of the solar cell parameters applied practically (using Kyocera KC175GHT PV modules) to test the proposed PV model, and were simulated in the Matlab environment, where the electrical characteristic of the Kyocera KC175GHT module are summarized in Table 1. In addition to the effect of cell temperature and solar irradiance level on the I–V and P–V characteristics, this part explains the influence of solar cell parameters on the I–V and P–V characteristic curves. The main parameters of

interest are the photocurrent,  $I_{ph}$ , the reverse diode saturation current,  $I_o$ , the ideality factor of diode,  $a$ , the series resistance,  $R_S$ , and the shunt resistance,  $R_{Sh}$ . In this section, the influence of these five parameters is deduced and the improvement of these parameters performance during its characteristics (I–V and P–V characteristics) are noticed, then its accuracy realized by comparing it with different models at the standard test conditions ( $G=1000\text{w/m}^2$ ,  $T=25^\circ\text{C}$ ).

#### 4.1. Effect of photocurrent, $I_{ph}$

The authors has implemented each solar cell parameter alone to show the influence of improvement of these five parameters on the I–V and P–V characteristic curves and then on the maximum power point (MPP), one by one simulated and its results presented in Figures (6-13). The first parameter in consideration was the photocurrent,  $I_L$ . The results of influence this parameter on both of I–V and P–V characteristic curves are presented in Figures 6 and 7, respectively.

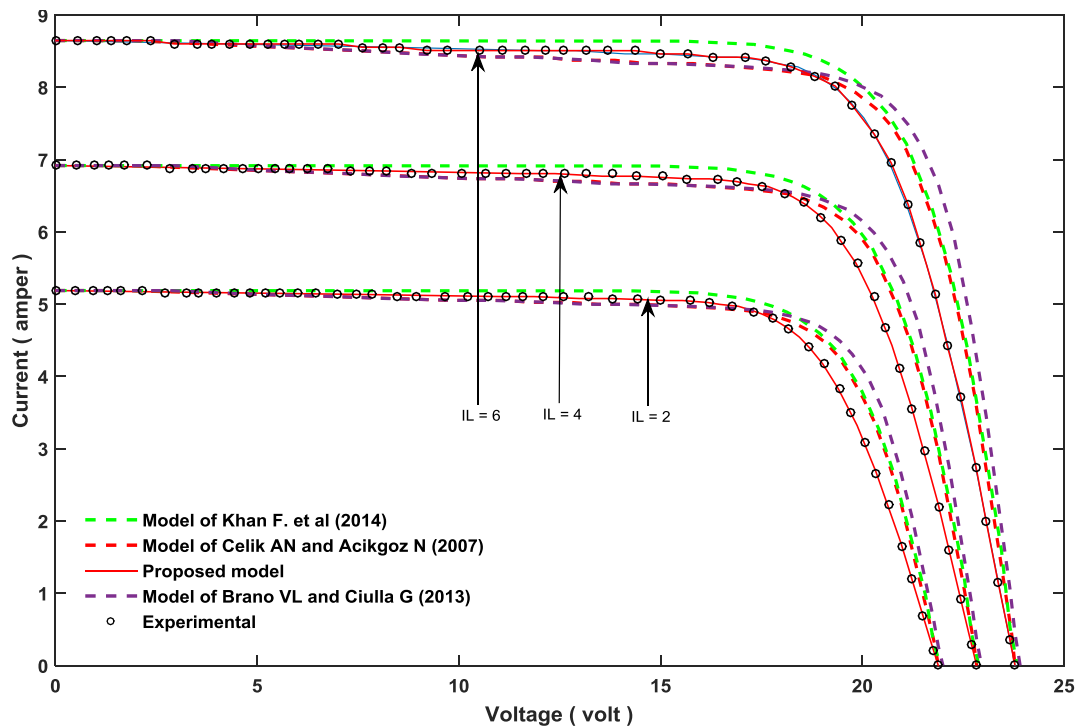


Figure 6. Influence of changing increasing  $I_{ph}$  on the I–V characteristic curve, at standard test condition ( $1000\text{ W/m}^2$ ,  $25^\circ\text{C}$ )

From Figures 6 and 7 we can deduce that the results given by the different models are in concordance with the proposed model and the experimental results of both of the I–V and P–V

characteristics. However, based on more than one benchmark subjected in this study, accuracy of the proposed model and its fitting to the experimental results is higher than all of the other compared models. The results of accuracy are presented in Table 4.

In addition, one can see from these Figures that the increasing in the photocurrent,  $I_{ph}$  leads to increase the maximum power point in a prominent way, besides to its effect on the short circuit current,  $I_{sc}$  and open circuit voltage,  $V_{oc}$ . This effect is also positively, since when increasing the  $I_{ph}$  it is lead to increase both of the  $I_{sc}$  and  $V_{oc}$ , but  $I_{sc}$  is affected more than the  $V_{oc}$  by this increasing.

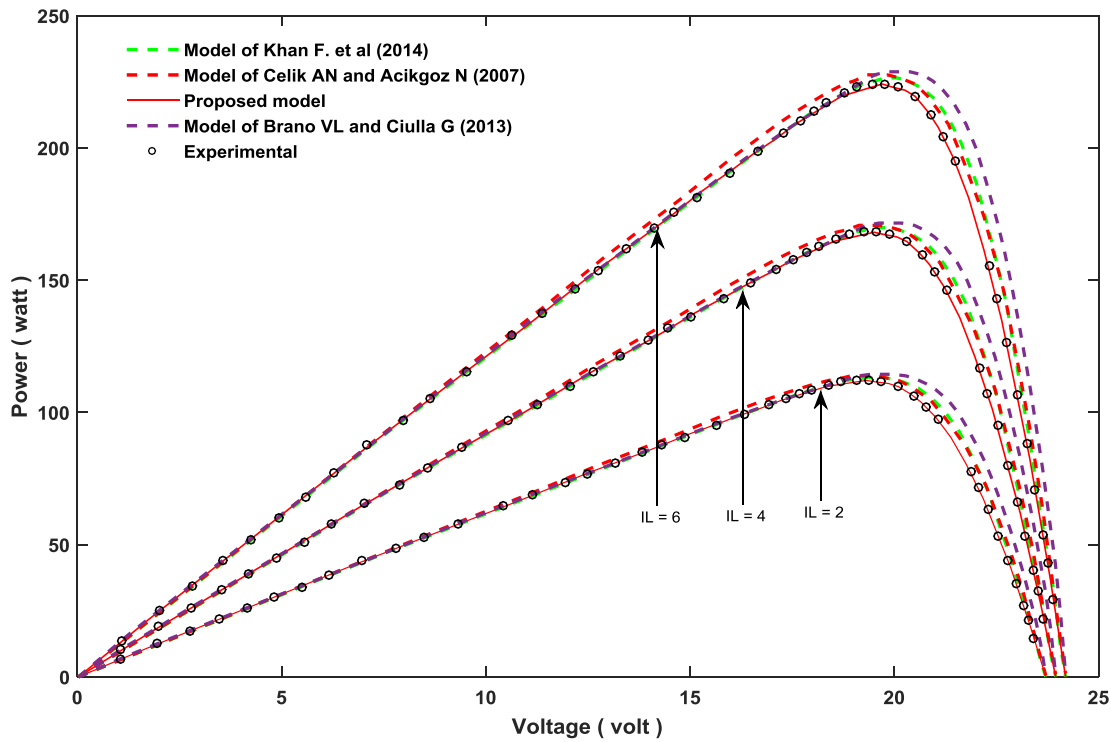


Figure 7. Influence of changing increasing  $I_{ph}$  on the P–V characteristic curve, at standard test condition ( $1000 \text{ W/m}^2, 25\text{C}^\circ$ )

#### 4.2. Effect of reverse diode saturation current, $I_o$

The second parameter in consideration for this study is the reverse diode saturation current,  $I_o$ . In the same condition of cell temperature and radiance value ( $1000 \text{ W/m}^2$ ,  $25\text{C}^\circ$ ) is applied also to carry out the influence of  $I_o$  on both of the I–V and P–V characteristic curves. The results of effect this parameter on the I–V and P–V characteristic curves are presented in Figures 8 and 9, respectively.

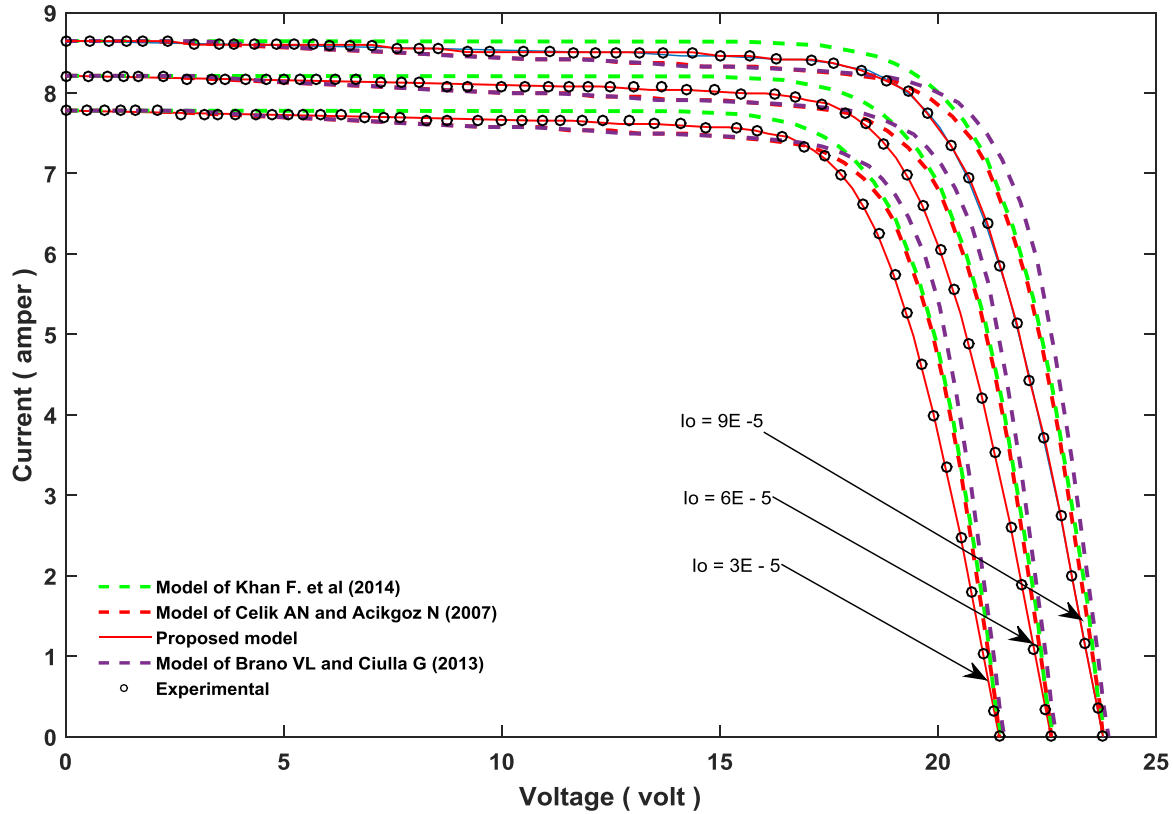


Figure 8. Influence of changing reverse diode saturation current,  $I_o$  on the I–V characteristic curve, at standard test condition ( $1000 \text{ W/m}^2$ ,  $25\text{C}^\circ$ )

From Figures 8 and 9 it can be seen that the results of the proposed model distinct in a high convergence fitting with the experimental results compared with the other selected models in this study [12, 20, 21], and for both of the I–V and P–V characteristics. Furthermore, based on more than one benchmark subjected in this study, the accuracy of the proposed model and it is fitting to the experimental results are higher than of all of the other compared models. The results of the accuracy of these models with the proposed model are existing in Table 4 likewise.

Moreover, these Figures deduced that the increasing in the reverse diode saturation current,  $I_o$  leads to increase the maximum power point in an average mode; in addition to that it is effect on the short circuit current,  $I_{sc}$  and open circuit voltage,  $V_{oc}$  too. This effect is also in a positive way. Further, when

increasing the reverse diode saturation current,  $I_o$  leads to increase both of the  $I_{sc}$  and  $V_{oc}$ , notice both of the  $I_{sc}$  and  $V_{oc}$  are affected by the same weight approximately.

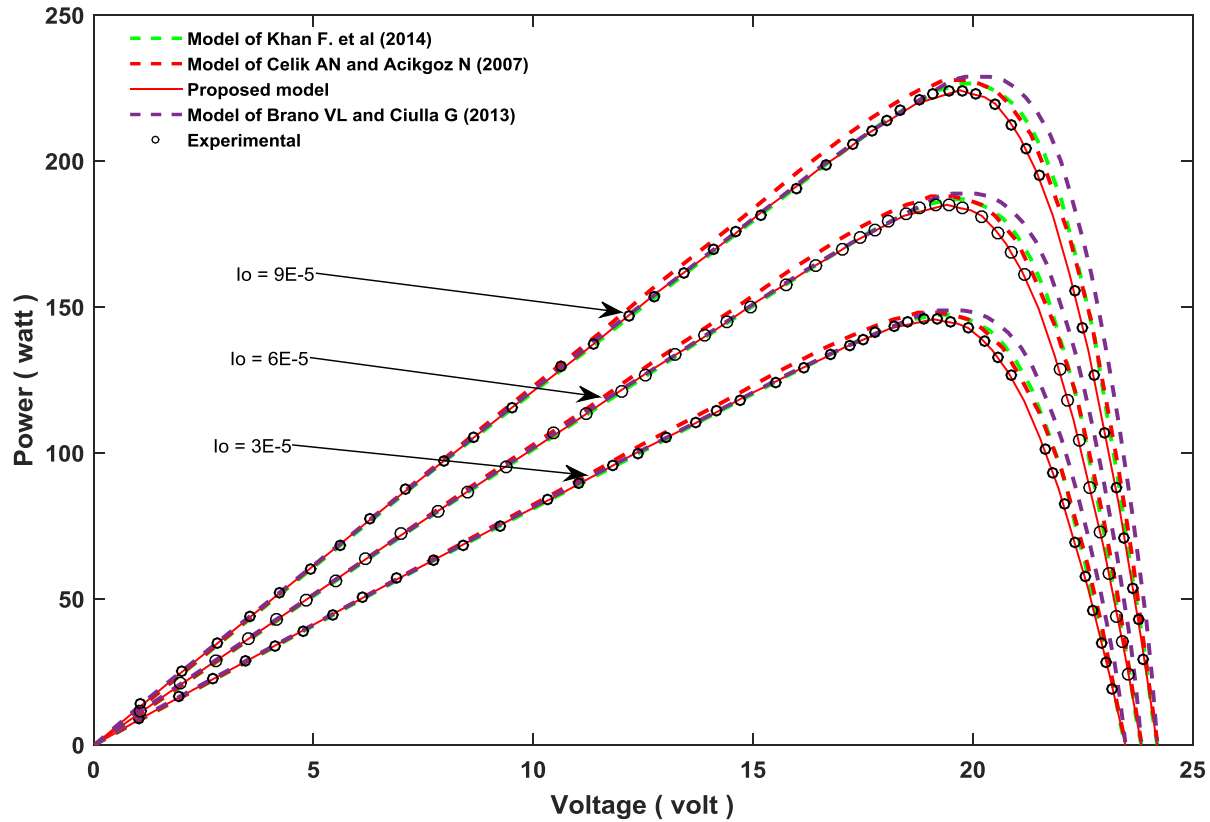


Figure 9. Influence of changing reverse diode saturation current,  $I_o$  on the P–V characteristic curve, at standard test condition ( $1000 \text{ W/m}^2$ ,  $25\text{C}^\circ$ )

#### 4.3. Effect of reverse diode ideality factor, $n$

The ideality factor parameter,  $n$  depends mainly on cell temperature, rather than irradiance level. Investigation of this parameter effect on the I–V and P–V characteristic curves with available real results and comparing with other models [12, 20, 21] were done in this study. This was done when the cell temperature and irradiance level were kept constant at standard test condition ( $1000 \text{ W/m}^2$ ,  $25\text{C}^\circ$ ). The results of the effect of this parameter on the I–V and P–V characteristic curves are presented in Figures 10 and 11, respectively.



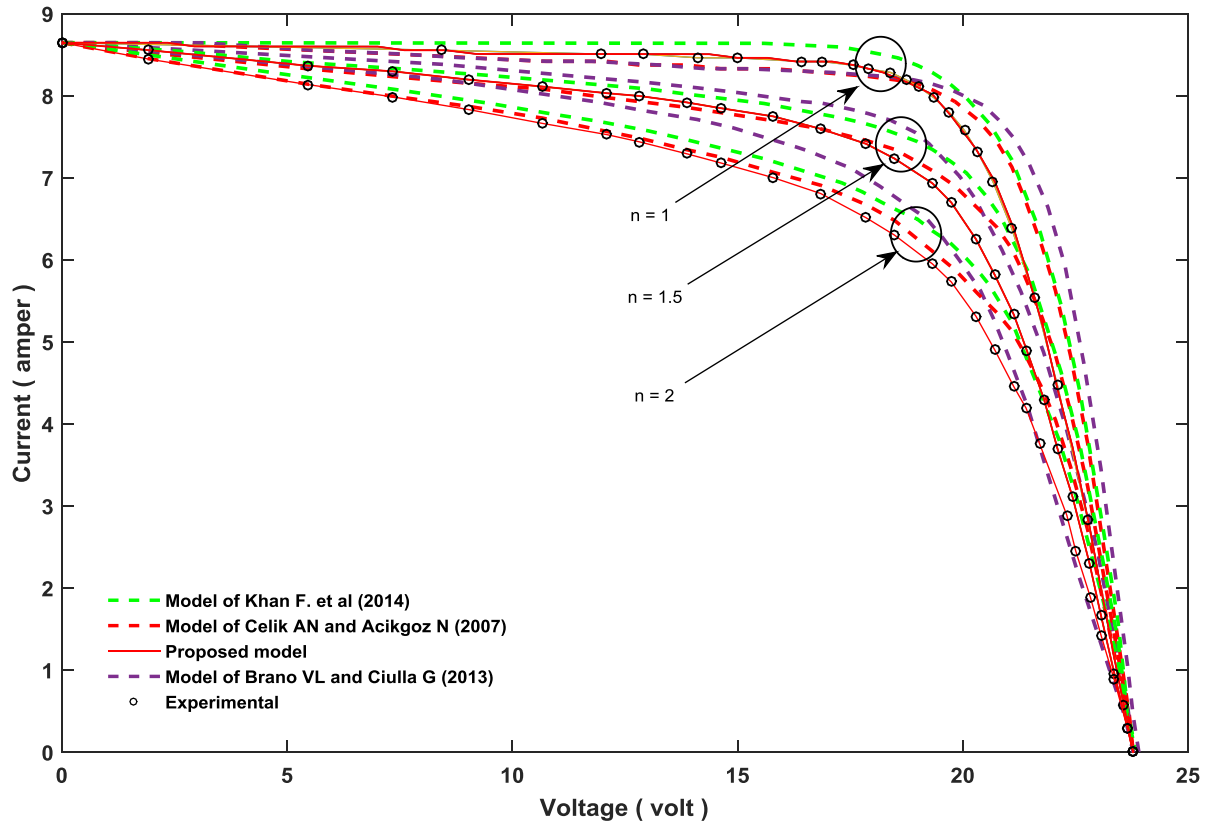


Figure 10. Influence of changing diode ideality factor,  $n$  on the I–V characteristic curve, at standard test condition ( $1000 \text{ W/m}^2$ ,  $25\text{C}^\circ$ )

The results obtained from Figures 10 and 11 showed that the changing of the diode ideality factor,  $n$  did not affect the values of the short circuit current  $I_{sc}$  and open circuit voltage  $V_{oc}$ . On the other hand, it is shown that the increasing in the diode ideality factor,  $n$  leads to decrease the value of the maximum power point for both of the I–V and P–V characteristic curves.

The results of effect the diode ideality factor on the I–V and P–V characteristic curves derived by simulation are compared with those of the experiment and . In terms of accuracy of the results, the exactness of obtained results for the different diode ideality factor (2, 1.5, and 1) is variable from one model to another, where the Celik AN and Acikgoz N model is strongly influenced by the variation of  $n$ . On the other hand, the proposed model keeps its performances well, regardless of variations in  $n$  values. However, the rest compared models were less affected than the Celik AN and Acikgoz N model.

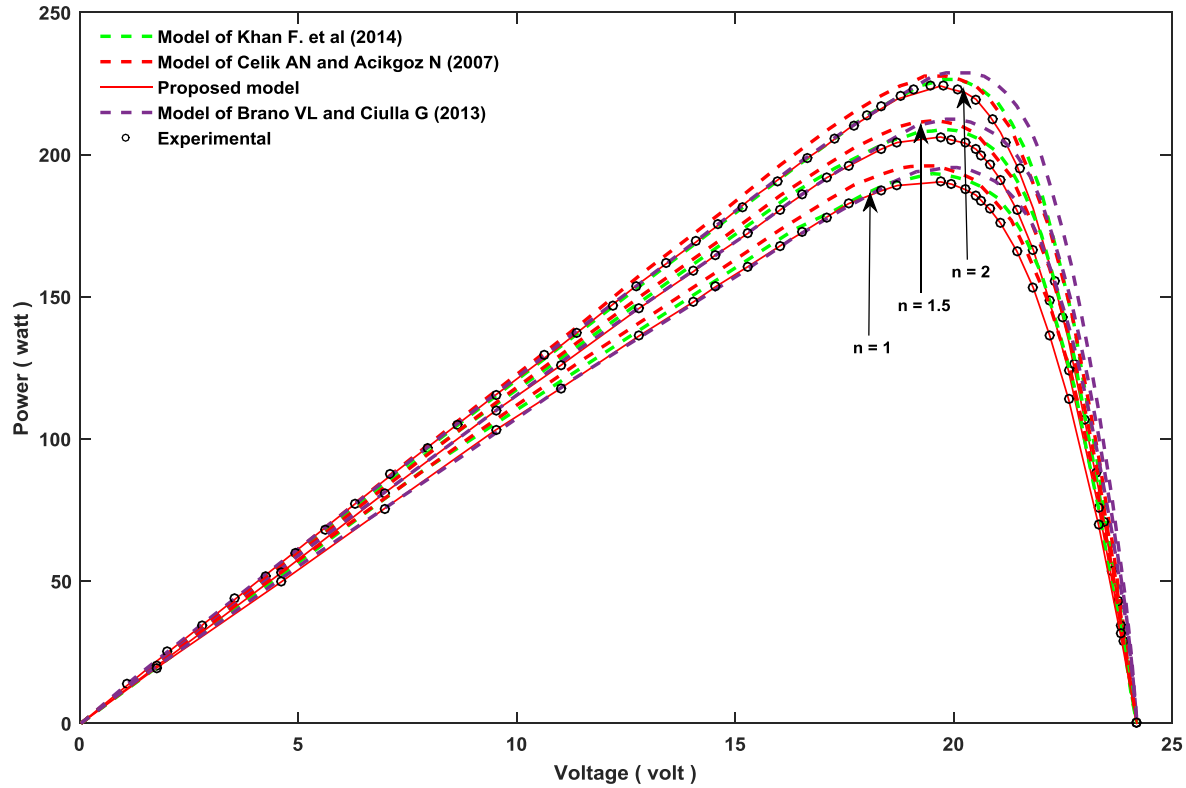


Figure 11. Influence of changing diode ideality factor,  $n$  on the I–V characteristic curve, at standard test condition ( $1000 \text{ W/m}^2$ ,  $25\text{C}^\circ$ )

#### 4.4. Effect of series resistance

The series resistance,  $R_s$  is another important parameter has to be considered for calculation the I–V and P–V characteristic curves. It was observed to be depend on the effective solar irradiance,  $G$  and the cell temperature,  $T$ . It controls the location of the maximum power point, therefore controls the current and voltage at the maximum power point. Investigation of this parameter effect on the I–V and P–V characteristic curves is also with a real results and comparing to other models [12, 20, 21] was done. For the same conditions of other parameters, this test is done when the cell temperature and irradiance level were kept constant at standard test condition ( $1000 \text{ W/m}^2$ ,  $25\text{C}^\circ$ ). The results of the effect of this parameter on the I–V and P–V characteristic curves are presented in Figures 12 and 13, respectively.

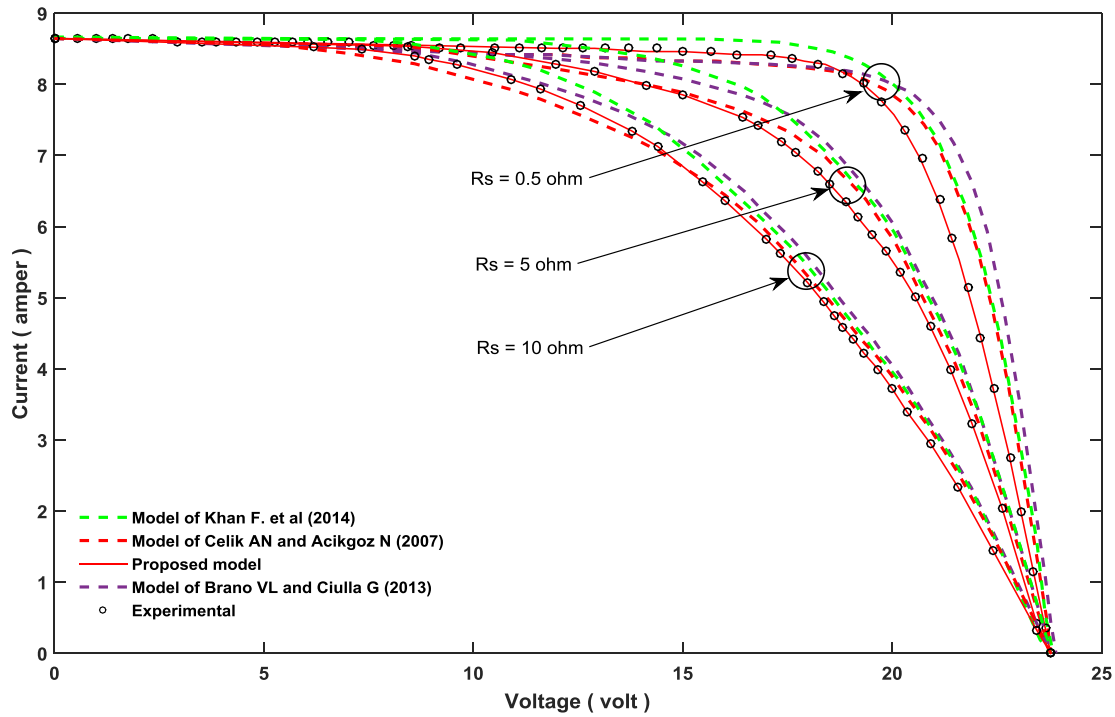


Figure 12. Influence of changing series resistance,  $R_s$  on the I-V characteristic curve, at standard test condition ( $1000 \text{ W/m}^2$ ,  $25\text{C}^\circ$ )

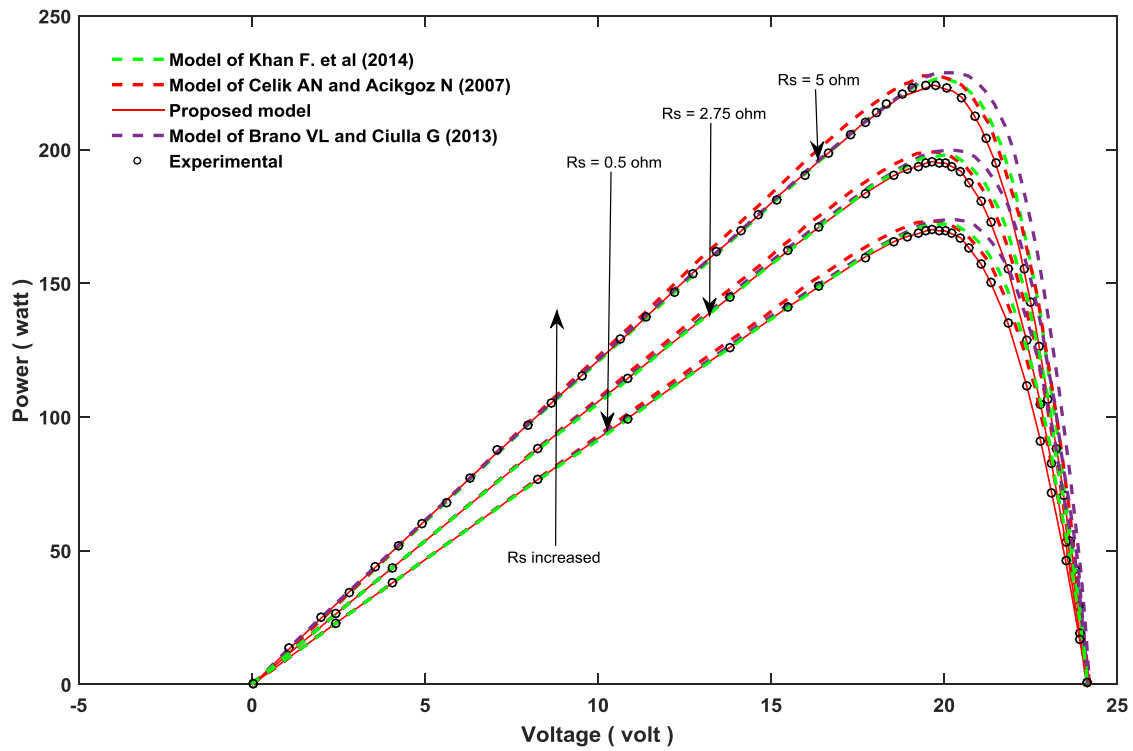


Figure 13. Influence of changing series resistance,  $R_s$  on the P-V characteristic curve, at standard test condition ( $1000 \text{ W/m}^2$ ,  $25\text{C}^\circ$ )

As introduced above, Figures 12 and 13 present the effect of the increasing of the value of the series resistance,  $R_s$  on the I–V and P–V characteristic curves. This results show that the increasing of the  $R_s$  do not affect the values of the short circuit current  $I_{sc}$  and open circuit voltage  $V_{oc}$ . On the other hand, it is showed that the increasing in  $R_s$  leads to decrease the value of the maximum power point notably, and for both of the I–V and P–V characteristic curves.

Furthermore, the results of the effect of the series resistance on the I–V and P–V characteristic curves are also like the other parameters derived by simulation and compared with those of the experiment and other models [12, 20, 21]. Finally, the accuracy of the results proves the exactness of the proposed model and for the different series resistance values (5, 3, and 0.5).

Table 4. Evaluation of Parameter performance based on accauracy level and models

Parameter Accuracy Based on Model	Model of F Khan		Model of Brano VL		Model of Celik AN		Proposed model	
	MAPE (%)	R-square	MAPE (%)	R-square	MAPE (%)	R-square	MAPE (%)	R-square
Effect of photocurrent, $I_L$	4.35 (%)	0.9843	5.18 (%)	0.9885	3.87 (%)	0.9887	0.85 (%)	0.99873
Effect of diode current, $I_o$	5.34 (%)	0.9823	6.15 (%)	0.9839	4.74 (%)	0.9858	0.94 (%)	80.99842
Effect of diode idealiry factor, $n$	4.28 (%)	0.9855	4.95 (%)	0.9874	4.27 (%)	0.9865	1.05 (%)	0.998242
Effect of series resistance, $R_s$	4.11 (%)	0.9865	5.37 (%)	0.9813	4.83 (%)	0.9847	0.35 (%)	0.999432
Effect of shunt resistance, $R_{sh}$	-----	-----	-----	-----	-----	-----	-----	-----

#### 4.5. Effect of parallel resistance

Finally, the fifth and the last parameter of interest was the shunt resistance,  $R_{sh}$ . In this purpose, the effect of varying parallel resistance,  $R_{sh}$  on the I–V and P–V characteristic curves of a PV module were also considered in this study. However, influence of this parameter found to be barely noticeable and for all of the maximum power point,  $I_{sc}$ , and  $V_{oc}$ .

#### References

- [1] A. M. Humada, F. B. Samsuri, M. Hojabria, M. B. Mohamed, M. H. B. Sulaiman, and T. H. Dakheel, "Modeling of photovoltaic solar array under different levels of partial shadow conditions," in *Power Electronics and Motion Control Conference and Exposition (PEMC), 2014 16th International*, 2014, pp. 461-465.

- [2] A. M. Humada, M. Hojabri, M. B. Mohamed, B. Sulaiman, M. Herwan, and T. H. Dakheel, "A Proposed Method of Photovoltaic Solar Array Configuration under Different Partial Shadow Conditions," in *Advanced Materials Research*, 2014, pp. 307-311.
- [3] A. M. Humada, M. Hojabri, S. Mekhilef, and H. M. Hamada, "Solar cell parameters extraction based on single and double-diode models: A review," *Renewable and Sustainable Energy Reviews*, vol. 56, pp. 494-509, 2016.
- [4] A. M. Dizqah, A. Maheri, and K. Busawon, "An accurate method for the PV model identification based on a genetic algorithm and the interior-point method," *Renewable Energy*, vol. 72, pp. 212-222, 2014.
- [5] G. Cibira and M. Koščová, "Photovoltaic module parameters acquisition model," *Applied Surface Science*, 2014.
- [6] R. Khezzar, M. Zereg, and A. Khezzar, "Modeling improvement of the four parameter model for photovoltaic modules," *Solar Energy*, vol. 110, pp. 452-462, 2014.
- [7] M. Ismail, M. Moghavvemi, and T. Mahlia, "Characterization of PV panel and global optimization of its model parameters using genetic algorithm," *Energy Conversion and Management*, vol. 73, pp. 10-25, 2013.
- [8] K. Ishaque and Z. Salam, "An improved modeling method to determine the model parameters of photovoltaic (PV) modules using differential evolution (DE)," *Solar Energy*, vol. 85, pp. 2349-2359, 2011.
- [9] G. Ciulla, V. L. Brano, V. Di Dio, and G. Cipriani, "A comparison of different one-diode models for the representation of I-V characteristic of a PV cell," *Renewable and Sustainable Energy Reviews*, vol. 32, pp. 684-696, 2014.
- [10] W. M. Keogh, A. W. Blakers, and A. Cuevas, "Constant voltage I-V curve flash tester for solar cells," *Solar Energy Materials and Solar Cells*, vol. 81, pp. 183-196, 2004.
- [11] V. L. Brano, A. Orioli, G. Ciulla, and A. Di Gangi, "An improved five-parameter model for photovoltaic modules," *Solar Energy Materials and Solar Cells*, vol. 94, pp. 1358-1370, 2010.
- [12] A. N. Celik and N. Acikgoz, "Modelling and experimental verification of the operating current of mono-crystalline photovoltaic modules using four-and five-parameter models," *Applied energy*, vol. 84, pp. 1-15, 2007.
- [13] D. S. Chan and J. C. Phang, "Analytical methods for the extraction of solar-cell single-and double-diode model parameters from IV characteristics," *IEEE Transactions on Electron Devices*, pp. 286-293, 1987.
- [14] E. Ortiz-Rivera and F. Z. Peng, "Analytical model for a photovoltaic module using the electrical characteristics provided by the manufacturer data sheet," in *Power Electronics Specialists Conference, 2005. PESC'05. IEEE 36th*, 2005, pp. 2087-2091.
- [15] D. Cotfas, P. Cotfas, and S. Kaplanis, "Methods to determine the dc parameters of solar cells: A critical review," *Renewable and Sustainable Energy Reviews*, vol. 28, pp. 588-596, 2013.
- [16] N. Kaushika, N. K. Gautam, and K. Kaushik, "Simulation model for sizing of stand-alone solar PV system with interconnected array," *Solar Energy Materials and Solar Cells*, vol. 85, pp. 499-519, 2005.
- [17] J. Shi, J. Dong, S. Lv, Y. Xu, L. Zhu, J. Xiao, *et al.*, "Hole-conductor-free perovskite organic lead iodide heterojunction thin-film solar cells: High efficiency and junction property," *Applied Physics Letters*, vol. 104, p. 063901, 2014.
- [18] G. Cibira and M. Koščová, "Photovoltaic module parameters acquisition model," *Applied Surface Science*, vol. 312, pp. 74-80, 2014.
- [19] K. Khouzam and K. Hoffman, "Real-time simulation of photovoltaic modules," *Solar Energy*, vol. 56, pp. 521-526, 1996.

- [20] F. Khan, S.-H. Baek, and J. H. Kim, "Intensity dependency of photovoltaic cell parameters under high illumination conditions: An analysis," *Applied Energy*, vol. 133, pp. 356-362, 2014.
- [21] V. L. Brano and G. Ciulla, "An efficient analytical approach for obtaining a five parameters model of photovoltaic modules using only reference data," *Applied Energy*, vol. 111, pp. 894-903, 2013.
- [22] W. Gong and Z. Cai, "Parameter extraction of solar cell models using repaired adaptive differential evolution," *Solar Energy*, vol. 94, pp. 209-220, 2013.
- [23] N. Rajasekar, N. Krishna Kumar, and R. Venugopalan, "Bacterial Foraging Algorithm based solar PV parameter estimation," *Solar Energy*, vol. 97, pp. 255-265, 2013.
- [24] A. Ortiz-Conde, F. J. G. Sánchez, and J. Muci, "New method to extract the model parameters of solar cells from the explicit analytic solutions of their illuminated I-V characteristics," *Solar Energy Materials and Solar Cells*, vol. 90, pp. 352-361, 2006.
- [25] M. S. El-Dein, M. Kazerani, and M. Salama, "Optimal photovoltaic array reconfiguration to reduce partial shading losses," *Sustainable Energy, IEEE Transactions on*, vol. 4, pp. 145-153, 2013.